ARTICLE

# Imidazolium Ionic Liquids As Antiwear and Antioxidant Additive in Poly(ethylene glycol) for Steel/Steel Contacts

**Meirong Cai,[†,†] Yongmin Liang,*[,†] Meihuan Yao,[†,†] Yanqiu Xia,[†] Feng Zhou,*[,†] and Weimin Liu*[,†]**

State Key Laboratory of Solid Lubrication, Lanzhou Institute of Chemical Physics, Chinese Academy of Sciences, Lanzhou 730000, China, Graduate School of Chinese Academy of Sciences, Beijing 100039, China

**ABSTRACT** Three imidazolium-based ionic liquids containing sterically hindered phenol groups were synthesized. The cation was 1-(3,5-ditert-butyl-4-hydroxybenzyl)-3-methyl-imidazolium, and the anions were tetrafluoroborates, hexafluorophosphates, and bis(trifluoromethylsulfonyl)imide. The physical properties of the synthetic products and of poly(ethylene glycol) (PEG) with the additive were evaluated. The oxidative stability of 0.5 wt % 1-(3,5-di-*tert*-butyl-4-hydroxybenzyl)-3-methyl-imidazolium hexafluorophosphates in PEG were assessed via rotating bomb oxidation test (RBOT), thermal analysis, and copper strip test. The tribological behaviors of the additives for PEG application in steel/steel contacts were evaluated on an Optimol SRV-IV oscillating reciprocating friction and wear tester as well as on MRS-1J four-ball testers. The worn steel surface was analyzed by a JSM-5600LV scanning electron microscope and a PHI-5702 multifunctional X-ray photoelectron spectrometer. RBOT test, thermal analysis, and copper strip test results revealed that synthesized ionic liquids possessed excellent antioxidant properties. Tribological application results revealed that these could effectively reduce friction and wear of sliding pairs compared with the PEG films used without the additives. Specifically, (BHT-1)MIMPF$_6$ exhibited better antiwear properties at an optimum concentration of 1 wt %. At this level, its antiwear property significantly improved by 100 times with respect to using just the PEG base oil. Boundary lubrication films composed of metal fluorides, organic fluorines, organic phosphines, and nitride compounds were formed on the worn surface, which resulted in excellent friction reduction and antiwear performance.

**KEYWORDS:** Ionic liquids • sterically hindered phenol • antiwear additives antioxidation additives • tribological properties

## 1. INTRODUCTION

Ionic liquids (ILs) are composed of organic cation and weakly coordinating anion salts with considerably low melting points (<100 °C) (1). They generate significant research interest because of their unique properties, including high thermal stability, nonvolatility, nonflammability, high ionic conductivity, wide electrochemical window, and miscibility with organic compounds (2, 3). Such interest has resulted in a significant number of studies spanning various fields, such as solvents in electrochemistry, organic synthesis, catalysis, separation science, biology, and materials for optoelectronic applications (4–9). Their characteristics are in sync with the demands for high-performance lubricants, including high thermal stability and nonvolatility.

ILs have attracted considerable attention in tribology (10) because their remarkable lubrication and antiwear (AW) capability is an improvement over average lubrication oils (11). ILs can be utilized as neat lubricants and additives, as thin films (12–23), and as components in polymer nanocomposites (24). Before this can be applied in practice, however, a number of issues need to be addressed (11), foremost of which is self-oxidation. To date, antioxidant ILs have never been reported, even for the most popular applications. This study reports a new series of antioxidant ILs and their use as AW and antioxidant additives in poly(ethylene glycol) (PEG) for steel/steel contacts.

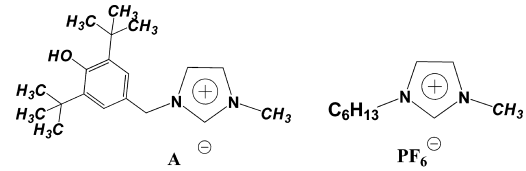


**FIGURE 1. Molecular structures of ILs: (a) (BHT-1)MIMPF$_6$, A = PF$_6$; (BHT-1)MIMNTf$_2$, A = N(CF$_3$SO$_2$)$_2$; (BHT-1)MIMBF$_4$, A = BF$_4$,; (b) L-P106.**

## 2. EXPERIMENTAL SECTION

**2.1. Chemicals.** Figure 1 presents the chemical structures of ILs: various kinds of 2,6-di-*tert*-Butyl-4-(chloromethyl)phenol and 1-methyl-3-hexyl-imidazolium hexafluorophosphates (L-P106), which were synthesized using previously reported methods (25, 26). The following reagents and materials were used as received: 2,6-di-*tert*-butyl phenol 98% (Alfa Aesar) and lithium bis(trifluoromethylsulfonyl)imide 99% (Fluka). The formaldehyde solution (37%−40%) was obtained from Tianjin Chemical Reagent No. 1 Plant. 1-Methylimidazole was obtained from Shanghai Weite Regent Company and redistilled before use. Sodium tetrafluoroborate and ammonium hexafluorophosphate were purchased from Shanghai Tongshi Regent Company

* Corresponding author. Tel.:+86-931-4968466. Fax: +86-931-8277088. E-mail: zhouf@lzb.ac.cn (F.Z.); wmliu@lzb.ac.cn (W.L.).
Received for review December 2, 2009 and accepted February 22, 2010
† Lanzhou Institute of Chemical Physics, Chinese Academy of Sciences.
† Graduate School of Chinese Academy of Sciences.
DOI: 10.1021/am900847j
© 2010 American Chemical Society


Published on Web 03/01/2010

**Table 1. Miscibility or Solubility of (BHT-1)MIMNTf$_2$, (BHT-1)MIMBF$_4$, and (BHT-1)MIMPF$_6$ with PEG Base Oil at Room Temperature**

| | (BHT-1)MIMNTf$_2$ | (BHT-1)MIMBF$_4$ | (BHT-1)MIMPF$_6$ |
|---|---|---|---|
| miscibility or solubility (weight fraction) | >50% | 4%−5% | 8%−10% |

and Shanghai Daocheng Regent Company, respectively. All other chemicals utilized in this work were of AR grade.

**2.2. Synthesis of 1-(3,5-Ditert-butyl-4-hydroxybenzyl)-3-methyl-imidazolium with Different Anions: Hexafluorophosphates [(BHT-1)MIMPF$_6$], (Trifluoromethylsulfonyl)-imide [(BHT-1)MIMNTf$_2$], and Tetrafluoroborates [(BHT-1)MIMBF$_6$].** *N*-Methylimidazole (1.642 g, 20 mmol) in THF (20 mL) was added to a solution of 2,6-di-*tert*-butyl-4-chloromethyl-phenol (5.096 g, 20 mmol) in THF (15 mL). After being stirred for approximately 15−20 h at room temperature, the reaction mixture was filtered to collect the white powder, which was dried in vacuum (yield: 3.577 g, 53.09%). Chloride salt (3.3690 g, 10 mmol) dissolved in 50 mL water was added to ammonium hexafluorophosphate (2.1199 g, 13 mmol). Anion exchange was allowed to proceed for 24 h at room temperature, afterwhich the reaction mixture was filtered to collect the white powder, which was dried in a vacuum (yield: 3.7280 g). The white powder was purified by silica gel column chromatography using 1:2 Sherwood oil/ethyl acetate as eluent. This resulted in a gray-white powder (Yield: 3.212 g, 71.9%). The structures of the prepared compounds were characterized by proton nuclear magnetic resonance ($^1$H NMR, 400 MHz) and carbon nuclear magnetic resonance ($^{13}$C NMR, 100 MHz) spectroscopy.

[(BHT-1)MIMPF$_6$]: $^1$H NMR ($CDCl_3$, 400 MHz), (ppm): 8.58 (s, 1H, N=CH), 7.26(s, 1H, NCH), 7.18 (s, 1H, CHN), 7.15 (s, 2H, arom), 5.15 (s, 2H, $CH_2$), 3.88 (s, 3H, $NCH_3$), 1.39 (s, 18H, $CCH_3$). $^{13}$C NMR ($CDCl_3$, 100 MHz), (ppm): 154.9, 137.1, 135.6, 126.12, 123.5, 122.9, 121.8, 54.0, 36.2, 34.3, 30.0.

[(BHT-1)MIMNTf$_2$]: $^1$H NMR ($CDCl_3$, 400 MHz), (ppm): 8.68(s, 1H, N=CH), 7.31 (s, 1H, NCH), 7.30 (s, 1H, CHN), 7.15 (s, 2H, arom), 5.41 (s, 1H, OH), 5.17 (s, 2H, $CH_2$), 3.90 (s, 3H, $NCH_3$), 1.40 (s, 18H, $CCH_3$). $^{13}$ C NMR ($CDCl_3$, 100 MHz), (ppm): 154.9, 137.1, 135.3, 126.0, 123.7, 122.8, 121.9, 121.3, 118.0, 53.9, 36.1, 34.2, 29.9.

[(BHT-1)MIMBF$_4$]: $^1$H NMR (DMSO-$d_6$, 400 MHz), (ppm): 9.12 (s, 1H, N=CH), 7.80 (s, 1H, NCH), 7.66 (s, 1H, CHN), 7.19 (s, 2H, arom), 7.162(s,1H,OH), 5.24 (s, 2H, $CH_2$), 3.83 (s, 3H, $NCH_3$), 1.36 (s, 18H, $CCH_3$). $^{13}$C NMR (DMSO-$d_6$, 100 MHz), (ppm): 154.4, 139.7, 136.1, 125.8, 125.3, 123.8, 122.2, 52.4, 35.7, 34.6, 30.2.

**2.3. Characterization.** PEG was purchased from Shanghai Chemical Reagent Company The average molecular weight was between 190−210 g/mol. Mixtures of base oil and additives were combined thoroughly prior to the tests. Table 1 presents the miscibility or solubility values. The IL (BHT-1)MIMNTf$_2$ had a solubility of 50% in PEG. The other two ILs with significant solubility can be used as additives as well. The density, viscosity, and viscosity-temperature index of the ILs were measured by a SVM3000 Stabinger viscometer (Table 2). The thermal properties of the PEG with ILs were measured on an STA 449 C Jupiter simultaneous TG-DSC from ambient temperatures to approximately 800 °C at a heating rate of 10 °C/min in air. The morphology and chemical composition of the worn surfaces were analyzed by JSM-5600LV SEM and PHI-5702 multifunctional XPS using Al K$\alpha$ radiation as exciting source. The binding energies of the target elements were determined at a pass energy of 29.35 eV with a resolution of approximately ±0.3 eV using the binding energy of the contaminated carbon (C1s: 284.6 eV) as reference.

**Table 2. Physical Properties of PEG and PEG with Different Additives**

| | kinematic viscosity (mm$^2$/s) | | viscosity | density (kg/m$^3$) |
|---|---|---|---|---|
| lubricant | 40 °C | 100 °C | index | at 25 °C |
| PEG | 22.59 | 4.20 | 78.6 | 1127.0 |
| 0.5% (BHT-1)MIMPF$_6$ | 22.98 | 4.22 | 75.5 | 1128.3 |
| 1% (BHT-1)MIMPF$_6$ | 23.53 | 4.35 | 86.1 | 1129.3 |
| 2% (BHT-1)MIMPF$_6$ | 24.18 | 4.36 | 78.4 | 1130.4 |
| 3% (BHT-1)MIMPF$_6$ | 25.00 | 4.45 | 79.2 | 1132.8 |
| 4% (BHT-1)MIMPF$_6$ | 25.74 | 4.60 | 87.9 | 1134.6 |
| 5% (BHT-1)MIMPF$_6$ | 26.67 | 4.56 | 86.2 | 1135.9 |
| 1% (BHT-1)MIMBF$_4$ | 23.97 | 4.33 | 77.2 | 1128.3 |
| 1% (BHT-1)MIMNTf$_2$ | 23.20 | 4.25 | 76.6 | 1129.5 |

**2.4. Oxidative Stability and Copper Strip Test.**

**2.4.1. *RBOT.*** The oxidative stability of the IL additives in PEG was evaluated by RBOT test using SH/T-0193 and ASTM D 2272 procedures. A total of 50 g of sample, 5 cm$^3$ of water, and catalytic copper wire were placed in an oxygen bomb. Oxygen was introduced at room temperature and 620 kPa initial pressure. The oxygen bomb was rotated at a rate of 100 rpm at 150 °C, and the oxygen pressure inside the reactor was monitored. The test was continued until the pressure reached a predetermined value. The test duration was reported as OIT, which characterized the oxidative stability of specimen.

**2.4.2. *Thermal Analysis.*** Thermal analysis is a popular method which involves measuring thermo-oxidative decomposition and temperature changes to study aging material and select antioxidants. The thermal behavior of the sample was carried outperformed on an STA 449 C Jupiter simultaneous TG-DSC. A total of 5 mg of sample was placed in the TGA sample holder. The temperature was programmed to increase from the initial temperature of 20 °C to approximately 400 °C, at a rate of 10 °C/min in air. The weight loss and heat flow values were monitored in the TG-DSC analysis.

**2.4.3. *Copper Strip Test.*** The test was performed using the GB-T5096−1985(91) procedure. A piece of bright finish copper was immersed within a certain amount of specimen. This was heated for 3 h at 100 °C. At the end of the test cycle, the copper was taken out after washing for comparison with the corrosion standard tint board.

**2.5. Tribology Test.** The tribological properties of the PEG film with additives were assessed for its application in steel/steel contacts using an Optimol SRV-IV oscillating reciprocating friction and wear tester, as well as MRS-1J four-ball testers. Friction and wear tests were performed at room temperature and at 100 °C, respectively, with a ball-on-block configuration. The contact between the frictional pairs was achieved by pressing the upper running ball (10 mm in diameter, AISI 52100 steel, hardness of approximately 59−61 HRC) against the lower stationary disk (ø 24 mm × 7.9 mm, AISI 52100 steel, hardness of approximately 58−60 HRC) at a frequency of 25 Hz, a sliding amplitude of 1 mm, a relative humidity of 30−40%, and for a duration of 30 min. The wear volume of the lower disk was measured using a MicroXAM 3D noncontact surface mapping profiler. Three repetitive measurements were performed for each disk and the reproducibility shown in Figure S1−Figure S4 in the Supporting Information as examples are very good.

The four-ball test was performed in a ball-on-ball configuration by oscillating an AISI52100 steel ball (12.7 mm in diameter) over three AISI52100 steel balls (12.7 mm in diameter) under the following conditions: rotating rate, 1450 rpm; duration, 30 min; load, 392N; and room temperature. The wear scar diameter (WSD) on the three lower balls was measured using an optical microscope, and friction coefficients were recorded

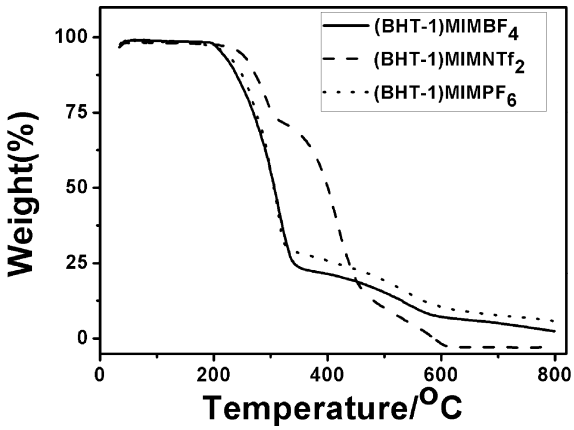


FIGURE 2. TGA curves of (BHT-1)MIMBF$_4$, (BHT-1)MIMNTf$_2$, and (BHT-1)MIMPF$_6$ in air atmosphere.

automatically by computer using a data-acquiring system linked to the four-ball tester.

## 3. RESULTS AND DISCUSSION

**3.1. Physical Properties of the Synthesized ILs.** The addition of ILs to PEG slightly increases its viscosity both at room temperature and at 100 °C (Table 2). The increase in viscosity is considerably concentration-dependent, which is the case for (BHT-1)MIMPF$_6$.

The TGA curves of ILs are presented in Figure 2. This clearly demonstrates that the ILs does not exhibit any weight loss below 200 °C. Furthermore, the temperature for total decomposition is approximately 600 °C, indicating that it has high thermal stability. The decomposition temperatures ($T_d$) are 219.8, 234.8, and 246.4 °C for (BHT-1)MIMBF$_4$, (BHT-1)MIMPF$_6$, and (BHT-1)MIMNTf$_2$, respectively. (BHT-1)MIMNTf$_2$ exhibited the best thermal stability.

**3.2. Oxidative Stability.** The oxidative stability of 0.5 wt % (BHT-1)MIMPF$_6$ in PEG is evaluated with the RBOT test. Addition of 0.5 wt % (BHT-1)MIMPF$_6$ into PEG results in 300 min of prolonged protection time. Meanwhile, the reference oil, PEG plus 0.5 wt % L-P106 fails to exhibit oxidative stability. The results reveal that phenol substitution does enhance the antioxidation properties of IL. The thermal behavior of the four ILs, in the form of 0.5 wt % additive in PEG, were measured using a STA 449 C Jupiter simultaneous TG-DSC from ambient temperatures to over 400 °C at a heating rate of 10 °C/min in air. The TG and DSC curves of the lubricants are presented in Figure 3.

The lubricants exhibited an exothermic decomposition peak due to the occurrence of endothermic oxidation. Thermo-oxidizing aging occurs in a single step. The oxidation and weight-loss temperatures of PEG shift higher after the addition of antioxidant IL. The details of the TG and DSC curves of the samples are listed in Table 3.

The thermo-oxidative decompositions for 0.5 wt % (BHT-1)MIMBF$_4$, 0.5 wt % (BHT-1)MIMNTf$_2$, and 0.5 wt % (BHT-1)MIMPF$_6$ in PEG are significantly improved and shifted higher by an increment of 90 °C compared to that of only PEG. The regular IL addition results in only a small increase in decomposition temperature.

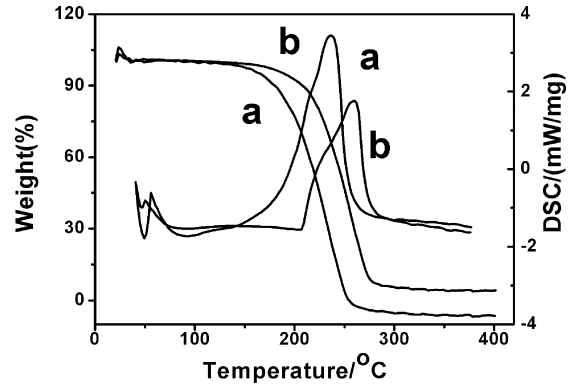


FIGURE 3. TGA and DSC curves of PEG and 0.5 wt % (BHT-1)MIMPF$_6$ additives in air: (a) PEG; (b) 0.5 wt % (BHT-1)MIMPF$_6$; (b) 0.5 wt % (BHT-1)MIMPF$_6$; (b) 0.5 wt % (BHT-1)MIMPF$_6$; (b) 0.5 wt % (BHT-1)MIMPF$_6$

Table 3. Performance Parameter for Lubricant

| lubricant | DSC initial thermo-oxidative decomposition temperature (°C) | TG temperature (°C) per weight loss 5% | 10% | 20% | copper strip test/corrosion grade |
|---|---|---|---|---|---|
| PEG | 117 | 165 | 180 | 196 | 1a |
| 0.5% (BHT-1)MIMBF$_4$ | 204 | 174 | 199 | 218 | 1a |
| 0.5% (BHT-1)MIMNTf$_2$ | 207 | 176 | 194 | 213 | 1a |
| 0.5% (BHT-1)MIMPF$_6$ | 208 | 187 | 209 | 224 | 1a |
| 0.5% L-P106 | 140 | 173 | 193 | 212 | 1a |

**3.3. Friction and Wear Behavior.** ***3.3.1. Effect of Additive Concentration.*** Figure 4a demonstrates the evolution of the friction coefficient with time at 100 N for [(BHT-1)MIMPF$_6$]+PEG with different additive concentrations and the wear volumes of the steel discs after testing. When the concentration of [(BHT-1)MIMPF$_6$] is merely 0.5 wt %, the mixture exhibits a friction behavior that is comparable to the base oil. Both have relatively long running-in time with larger friction coefficients. When the concentration of [(BHT-1)MIMPF$_6$] is above 1 wt %, the running-in time is dramatically shortened, concomitant with very stable friction and a lower friction coefficient. The wear volumes are significantly reduced upon addition of (BHT-1)MIMPF$_6$ above 1 wt %. After increasing the concentration of (BHT-1)MIMPF$_6$ above 1 wt %, no further improvement in AW property can be observed (Figure 4b). The addition of 1 wt % (BHT-1)MIMPF$_6$ can already improve the AW property of the base oil by 100 times.

***3.3.2. Effect of Temperature and Load.*** The effect of the temperature and load on the tribological behavior of 1−5 wt % (BHT-1)MIMPF$_6$ in PEG is shown in Figure 5. This is under the same test duration of 30 min and a frequency of 25 Hz, but the test is done at 100 °C. The mean friction coefficient and wear volume for PEG at 100 N and 100 °C are obviously larger compared with those at room temperature. However, for oil samples with 1−5 wt % (BHT-1)MIMPF$_6$, temperature has a negligible effect on the mean friction coefficient and wear volume. This indicates that (BHT-1)MIMPF$_6$ is capable of superior tribological performance at elevated temperatures. The addition of (BHT-1)MIMPF$_6$ considerably reduces the friction coefficients of base oil, especially under a high load (Figure 5a).

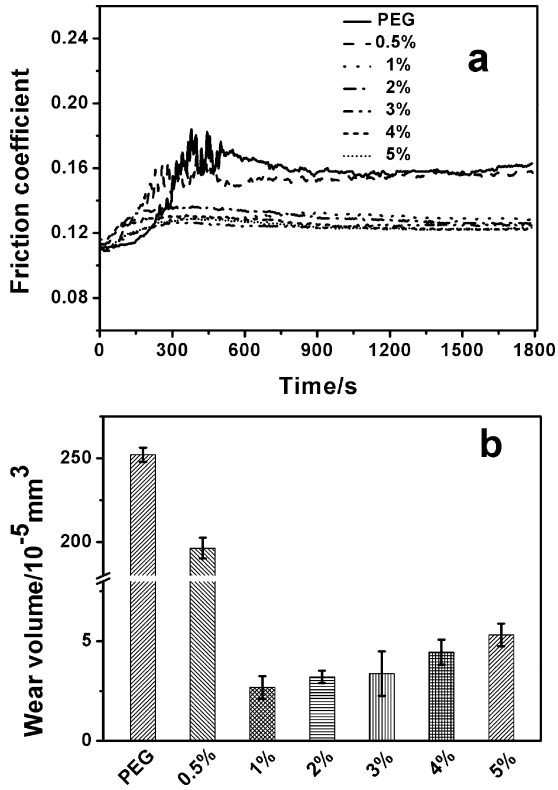


FIGURE 4. (a) Evolution of friction coefficient with time at 100 N for PEG plus (BHT-1)$MIMPF_6$ additive at different concentrations at room temperature; (b) wear volumes of the steel discs lubricated by PEG with (BHT-1)$MIMPF_6$ additive at different concentrations at room temperature (SRV load =100 N; stroke = 1 mm; frequency = 25 Hz; duration = 30 min).

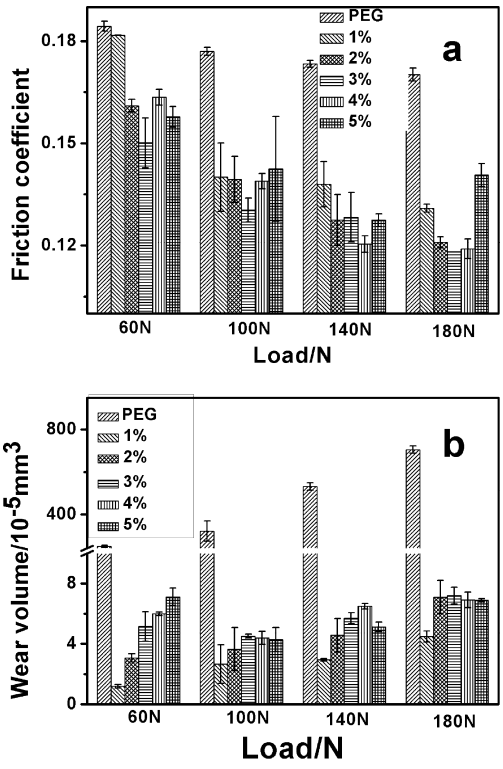


FIGURE 5. (a) Mean friction coefficients and (b) mean wear volumes at 60, 100, 140, and 180 N of steel/steel contacts lubricated with PEG and (BHT-1)$MIMPF_6$ additives at different concentrations at 100 °C (SRV stroke = 1 mm; frequency = 25 Hz; duration = 30 min).

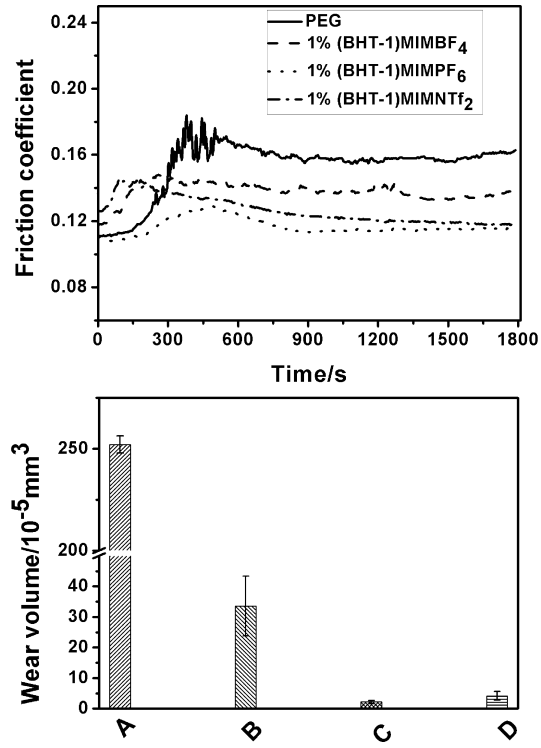


FIGURE 6. (a) Changes in the friction coefficient relative to time at 100 N for PEG and different IL additives at room temperature; (b) wear volumes of steel discs lubricated by PEG and different IL additives at room temperature (SRV load = 100 N; stroke = 1 mm; frequency = 25 Hz; duration = 30 min).

Figure 5b shows that the wear volumes of the steel discs lubricated with the oil mixture remain considerably lower at all loads compared with the base oil. An additive concentration of 1 wt % results in the best friction reduction and antiwear capability.

**3.4. Effect of Anion.** Figure 6 displays the changes in friction coefficients and wear volumes of sliding discs under lubrication with antioxidant ILs composed of different anions. The friction coefficients of the three PEG + additive mixtures increase in the following sequence: (BHT-1)$MIMPF_6$ < (BHT-1)$MIMNTf_2$ < (BHT-1)$MIMBF_4$< PEG. The wear volume of the discs increase in the following order: (BHT-1)$MIMPF_6$ < (BHT-1)$MIMNTf_2$ < (BHT-1)$MIMBF_4$ < PEG. The addition of 1 wt % (BHT-1)$MIMPF_6$, 1 wt % (BHT-1)$MIMNTf_2$, and 1 wt % (BHT-1)$MIMBF_4$ can improve the AW properties of the base oil by 113, 60, and 7.5 times, respectively. (BHT-1)$MIMPF_6$ clearly results in the best friction reduction and AW property. This may possibly be caused by their various capabilities to form effective boundary films and chemical reaction film (22, 27).

Figure 7 displays a load ramp test stepped from 50 N up to 300 N by 50 N intervals at a frequency of 25 Hz for three kinds of PEG+additive at room temperature. The test duration for each load is 5 min. It is evident that all oils experience a running-in period. Further, the three mixtures present lower friction coefficients most of the time compared with only the base oil. The frictional behaviors, as a function of load for PEG and 1 wt % (BHT-1)$MIMBF_4$, are quite similar. They fluctuate even at a later stage. (BHT-1)$MIMPF_6$ behaves similarly with (BHT-1)$MIMNTf_2$. With the

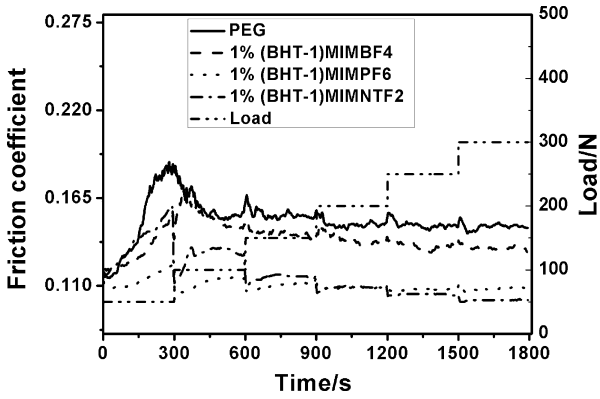


FIGURE 7. Evolution of friction coefficient with time during a load ramp test from 50 to 300 N for PEG and different IL additives at room temperature (SRV stroke = 1 mm; frequency = 25 Hz; duration = 30 min).

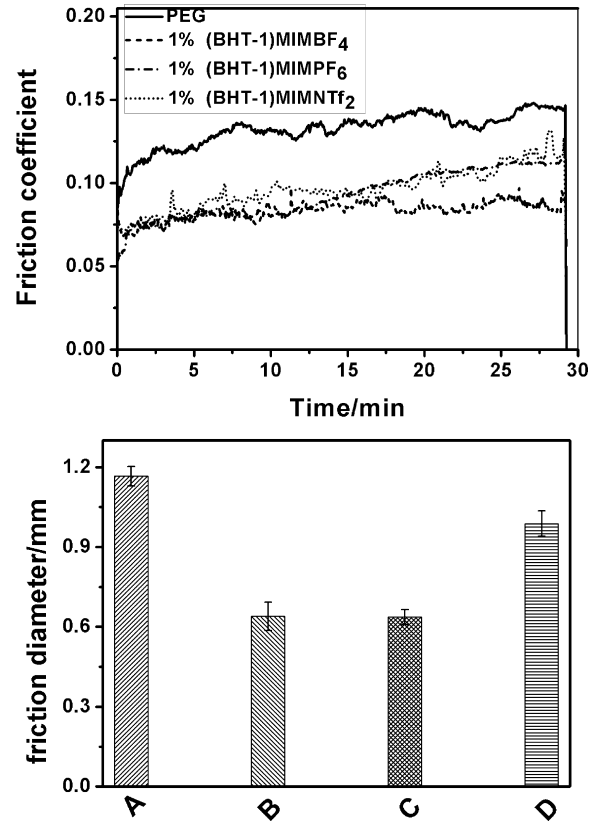


FIGURE 8. (a) Evolution of friction coefficient with time at 392 N for PEG and different IL additives at room temperature; (b) wear scar diameters of steel balls lubricated by PEG and different IL additives at room temperature (load = 392 N; rotating rate = 1450 rpm; duration = 30 min).

exception of the initial running-in period, they remain at a very stable friction state.

A standard four-ball tester is likewise employed to study the friction behavior of the additive in PEG at 392 N (Figure 8). The three mixtures present lower friction coefficients compared with pure PEG. The friction coefficients of the additives and PEG increased in the following sequence: (BHT-1)$MIMBF_4$ < (BHT-1)$MIMPF_6$ < (BHT-1)$MIMNTf_2$ < PEG, whereas the wear scar diameters of the steels balls increased in the following order: (BHT-1)$MIMBF_4$ = (BHT-1)$MIMPF_6$ < (BHT-1)$MIMNTf_2$ < PEG. This indicates that all three ILs are good additives for

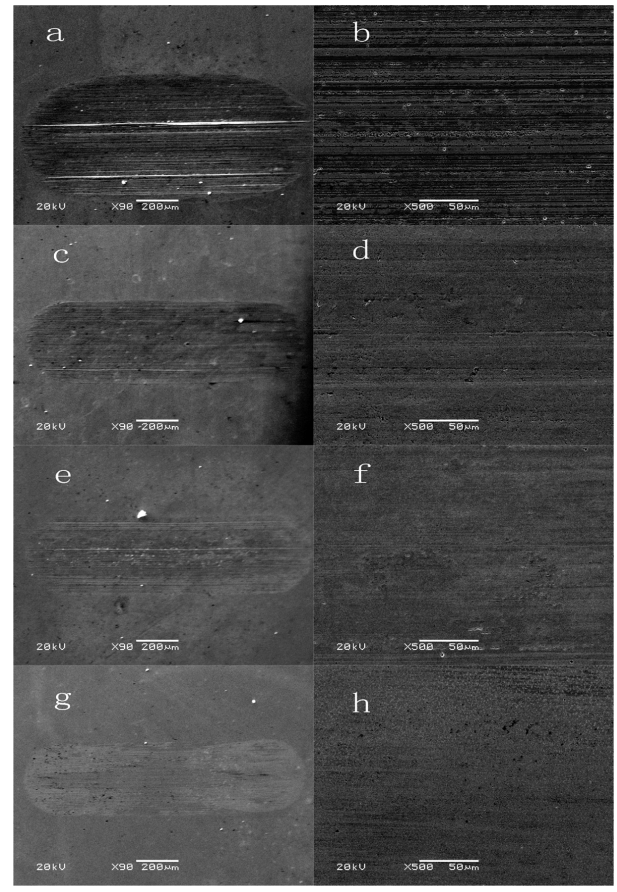


FIGURE 9. SEM morphologies of worn surfaces lubricated by PEG and different IL additives: (a, b) PEG, (c, d) 1 wt % (BHT-1) $MIMBF_4$, (e, f) 1 wt % (BHT-1) $MIMNTf_2$, and (g, h) 1 wt % (BHT-1) $MIMPF_6$, (magnification: on the left is 90×, and on the right is 500×; load = 100 N; stroke = 1 mm; frequency = 25 Hz; duration = 30 min).

improving the lubricating property of PEG. They exhibit outstanding friction reduction and AW properties. In particular, 1 wt % (BHT-1)$MIMPF_6$ and 1 wt % (BHT-1)$MIMBF_4$ result to more improvements in the tribological properties.

**3.5. Surface Analysis.** Figure 9 displays the SEM micrographs of the worn surfaces of steel discs lubricated by PEG and three additives at 100 N and 25 Hz. It is clearly seen that the worn surface of steel under PEG lubrication (Figure 9a, b) exhibits considerably wider and deeper wear scar, with a number of deep and narrow grooves. Thus, severe scuffing occurs in this case. As demonstrated in images c and d in Figure 9, the wear scars of steel discs lubricated by 1 wt % (BHT-1)$MIMBF_4$ are relatively narrow and shallow, and scuffing is greatly alleviated. In marked contrast, not only is the width of wear scars smaller in size for steel discs lubricated with 1 wt % (BHT-1)$MIMNTf_2$ and 1 wt % (BHT-1)$MIMPF_6$ but the abrasions are also fewer and smoother (Figure 9e–h). This is consistent with previously measured wear volume results.

To gain further insight into the lubricating mechanism of ILs, Figure 10 presents the XPS spectra. Table S1 in the Supporting Information provides the atomic percent on worn steel surfaces lubricated by three kinds of IL additives. Figure 10a–c (SRV at room temperature) and Figure 10g (SRV at 100 °C) display the XPS spectra of worn steel discs

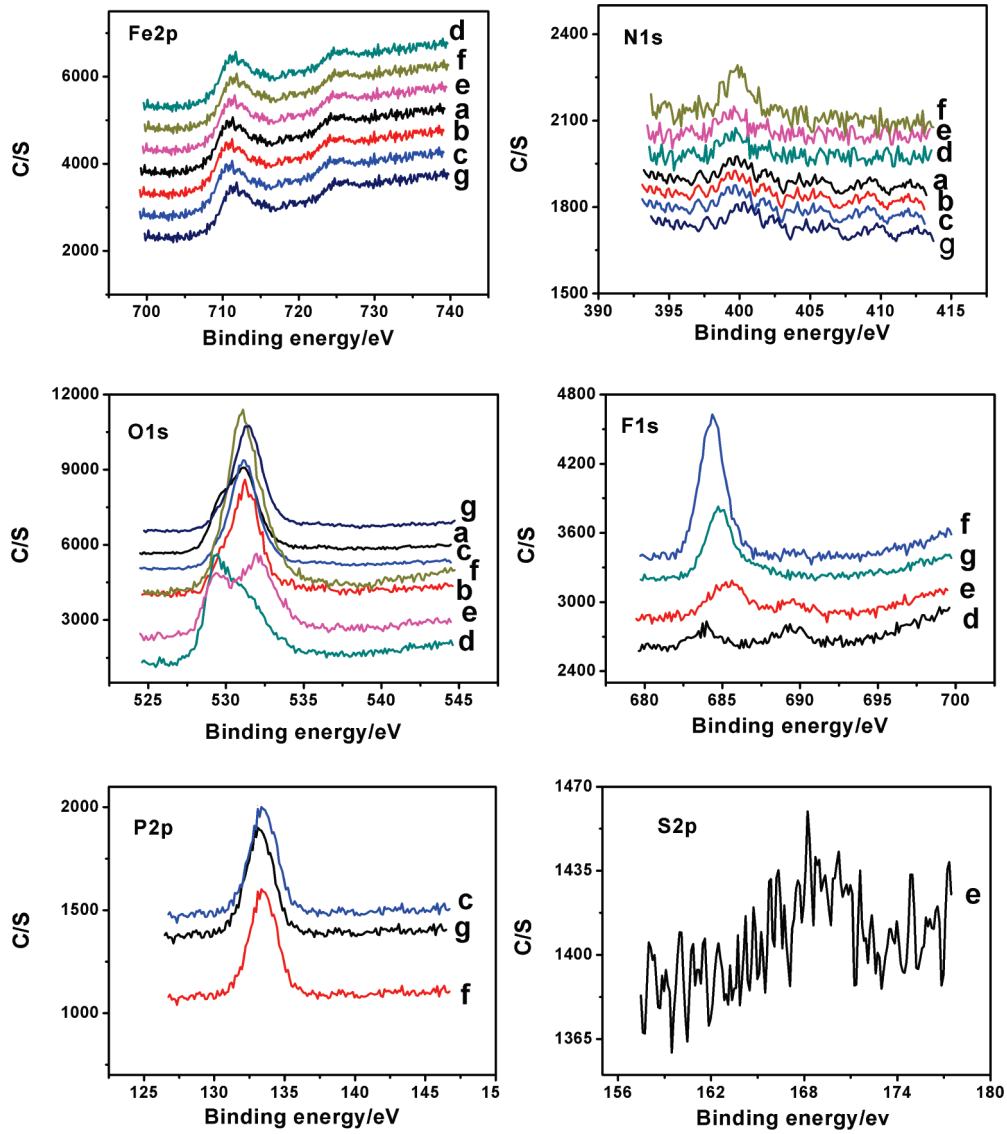


**FIGURE 10. XPS spectra of Fe2p, O1s, F1s, N1s, P2p, and S2p of worn surfaces lubricated by (a, d) 1 wt % (BHT-1)MIMBF$_4$, (b, e) 1 wt % (BHT-1)MIMNTf$_2$, and (c, f) 1 wt % (BHT-1)MIMPF$_6$ at room temperature, and (g) 1 wt %(BHT-1)MIMPF$_6$ at 100 °C.**

surfaces. Figure 10d−f (four-ball testers at room temperature) exhibit the XPS spectra of worn steel balls surfaces. The binding energies of all samples are presented in Table S2 in the Supporting Information.

Figure 10 reveals that the XPS peaks F1s varies within the range of 684−685.4 eV. These values indicate the presence of $F^-$, possibly due to the formation of ionic compounds, such as $FeF_2$ or $FeF_3$ (22, 28, 29). To determine the type of formation, we studied XPS peaks of Fe2p. Figure 10d−g shows the peak of Fe2p at approximately 711.4, 711.3, and 724 eV, which may correspond to $FeF_2$, $FeF_3$, Fe(OH)O, and $Fe_2O_3$ (30). Thus, with the existing conditions, it is difficult to determine the type of species. Apart from these iron fluorides, the presence of F1s peaks at higher binding energies (689.5 eV in Figures 10d−f) are ascribed to covalently bonded F (22). XPS peaks of Fe2p (Figures 10a−c) appear at the binding energies of 711.3 and 724 eV, which may correspond to Fe(OH)O and $Fe_2O_3$ (30). F1s cannot be detected on worn steel surfaces lubricated with all three kinds of IL additives. Almost no difference is observed in XPS peaks of N1s (Figure 10) on the worn surfaces. The N1s spectra are extremely wide, and the peak binding energies vary within the range of 399.7−400.2 eV, which may include C−N bonding and nitrogen trasformation to amine or nitrogen oxide (12, 22). P2p peaks appear at approximately 132.8 (Figure 10g), 133.3 (Figure 10f), and 133.0 eV (Figure 10c). After comparing these against the standard spectra of the elements (30), the presence of P can be identified at the worn surface and it can be assigned to organic phosphine. However, it is difficult to verify the covalently organic phosphine species. The XPS spectra of O1s (Figure 10) for worn steel surfaces lubricated by the three types of IL additives are more complicated. The O1s (Figure 10a−c, f) peaks are similar to each other, appearing at approximately 531.1 eV, which can be assigned to C−O and P−O bonding (30).

Figure 10g reveals that the O1s peak appearing at 531.4 eV may correspond to FeOOH (31). The O1s peak appears at approximately 532.0 eV. Combined with the binding energy of S2p at 168.7 eV, this indicates that tribochemical

reaction was involved in the generation of iron(III) sulfate or ferrous sulfate(II) (32). The characteristic absorption peaks of F1s (a, b, and c) and B1s could not be detected on worn steel surfaces lubricated with all three types of IL additives. Only very small amounts of sulfur are present on the wear surfaces lubricated with 1 % (BHT-1)MIMNTf$_2$ additive in the four-ball test.

XPS analysis reveals that apart from inorganic compounds (e.g., $Fe_2O_3$, $FeF_2$, $FeF_3$, FeOOH, amine or nitrogen oxide, iron(III) sulfate or ferrous sulfate (II) formed on the worn surfaces), organic phosphine, covalently bonded F, and C−N bonding can be present at the worn surface. On the basis of these data, Minami proposed a model where the rubbing surface is treated as a reaction zone (28). It can be speculated here that under a collective impact of high pressure, exoelectron emission, and frictional heat on the specimen surface, complicated tribochemical reactions can occur on the surfaces lubricated by all three types of IL and a surface protective film composed of $FeF_2$, $FeF_3$, iron(III) sulfate or ferrous sulfate, and organic phosphine can be generated on the lubricated metal surface.

## 4. CONCLUSIONS

A series of antioxidant imidazolium compounds containing sterically hindered phenol groups were synthesized for the first time. Their structures were characterized by $^1$H NMR (400 MHz) and $^{13}$C NMR (100 MHz) spectroscopy. Imidazolium ILs, (BHT-1)MIMBF$_4$, (BHT-1)MIMPF$_6$, and (BHT-1)MIMNTf$_2$, possess good miscibility with PEG as the base oil. RBOT test results revealed that synthesized ILs can serve as antioxidants in PEG, prolonged its lifespan by 300 min.

The thermal analysis likewise verified its antioxidation characteristics in PEG. The thermal decomposition temperature of PEG was lowered. The addition of 1 wt % (BHT-1)MIMPF$_6$ in PEG significantly reduced the friction coefficient and wear volume. XPS analysis revealed that complicated tribochemical reactions occurred during the friction process involving two different evaluation tools. Active elements in ILs, such as P, F, N, and S, might react with the disk surface to form a reactive film under the collective impact of high pressure, exoelectron emission, and frictional heat. A boundary lubrication film composed of metal fluorides, organic fluorines, organic phosphines, and nitride compounds were formed on the worn surface, leading to friction reduction and AW performance.

**Acknowledgment.** The authors are grateful for financial support of this work by "973" Program (2007CB607601), NSFC (50721602, 20533080), and Chinese Academy of Sciences (KJCX2.YW.H16).

## APPENDIX

### Nomenclature

| | |
|---|---|
| ASTM | American Society for Testing Materials |
| SH | petrochemical |
| GB | Chinese National Standard |
| SEM | scanning electron microscope |
| XPS | X-ray photoelectron spectroscopy |
| RBOT | rotary bomb oxidation test |
| OIT | oxidation induction time |
| TGA | thermogravimetric analysis |
| DSC | differential scanning calorimetry |
| NMR | nuclear magnetic resonance |
| WSD | wear scar diameters |
| PEG | poly(ethylene glycol) |
| BF4 | tetrafluoroborate |
| PF6 | Hhexafluorophosphate |
| NTf2 | bis(trifluoromethylsulfonyl)imide |
| AR | analytical reagent |

**Supporting Information Available:** Tables S1 and S2 listing XPS data in Figure 10; Figure S1−S4 listing repetitive tribological curves of different test runs (PDF). This material is available free of charge via the Internet at http://pubs.acs.org.

### REFERENCES AND NOTES

(1) Earle, M. J.; Seddon, K. R. *Pure Appl. Chem.* **2000**, *72*, 1391–1398.
(2) Hagiwara, R.; Ito, Y. *J. Fluorine Chem.* **2000**, *105*, 221–227.
(3) Wilkes, J. S. *Green Chem.* **2002**, *4*, 73–80.
(4) Welton, T. *Chem. Rev.* **1999**, *99*, 2071–2084.
(5) Davis Jr, J H.; Forrester, K J.; Merrigan, T. *Tetrahedron Lett.* **1998**, *39*, 8955–8958.
(6) Landini, D.; Maia, A. *Tetrahedron Lett.* **2005**, *46*, 3961–3963.
(7) Zhang, S.; Zhang, Q.; Zhang, Z. *Ind. Eng. Chem. Res.* **2004**, *43*, 614–622.
(8) Zhang, J.; Bond, A. M. *Anal. Chem.* **2003**, *75*, 2694–2702.
(9) Haristoy, D.; Tsiourvas, D. *Chem. Mater.* **2003**, *15*, 2079–2083.
(10) Ye, C. F.; Liu, W. M.; Chen, Y. X.; Yu, L. G. *Chem. Commun.* **2001**, *21*, 2244–2245.
(11) Zhou, F.; Liang, Y. M.; Liu, W. M. *Chem. Soc. Rev.* **2009**, *38*, 2590–2599.
(12) Wang, H. Z.; Lu, Q. M.; Ye, C. F.; Liu, W. M.; Cui, Z. J. *Wear* **2004**, *256*, 44–48.
(13) Lu, Q. M.; Wang, H. Z.; Ye, C. F.; Liu, W. M.; Xue, Q. J. *Tribol. Int.* **2004**, *37*, 547–552.
(14) Mu, Z. G.; Zhou, F.; Zhang, S. X.; Liang, Y. M.; Liu, W. M. *Tribol. Int.* **2005**, *38*, 725–731.
(15) Yu, G. Q.; Zhou, F.; Liu, W. M.; Liang, Y. M.; Yan, S. Q. *Wear* **2006**, *260*, 1076–1080.
(16) Liu, X. Q.; Zhou, F.; Liang, Y. M.; Liu, W. M. *Wear* **2006**, *261*, 1174–1179.
(17) Weng, L. J.; Liu, X. Q.; Liang, Y. M.; Xue, Q. J. *Tribol. Lett.* **2007**, *26*, 11–17.
(18) Yu, B.; Zhou, F.; Mu, Z. G.; Liang, Y. M.; Liu, W. M. *Tribol. Int.* **2006**, *39*, 879–887.
(19) Yao, M. H.; Liang, Y. M.; Xia, Y. Q.; Zhou, F. *ACS Appl. Mater. Interfaces* **2009**, *1*, 467–471.
(20) Jimenez, A. E.; Bermudez, M. D.; Iglesias, P.; Carri'on, F. J.; Martınez-Nicolas, G. *Wear* **2006**, *260*, 766–782.
(21) Jimenez, A. E.; Bermudez, M. D. *Wear* **2008**, *265*, 787–798.
(22) Hernández Battez, A.; González, R.; Viesca, J. L.; Blanco, D.; Asedegbega, E.; Osorio, A. *Wear* **2009**, *266*, 1224–1228.
(23) Qu, J.; Blau, P. J.; Dai, S.; Luo, H. M.; Meyer III, H. M. *Tribol. Lett.* **2009**, *35*, 181–189.
(24) Bermudez, M. D.; Jimenez, A. E.; Sanes, J.; Carrion, F. J. *Molecules* **2009**, *14*, 2888–2908.
(25) Neureiter, N. P. *J. Org. Chem.* **1963**, *28* (12), 3486–3490.
(26) Bonhote, P.; Dias, A. P.; Papageorgiou, N.; Kalyanasundaram, K.; Gratzel, M. *Inorg. Chem.* **1996**, *35*, 1168–1178.
(27) Kamimura, H.; Kubo, T.; Minami, I.; Mori, S. *Tribol. Int.* **2007**, *40*, 620–625.
(28) Minami, I. *Molecules* **2009**, *14*, 2286–2305.
(29) Sanders, J. H.; Cutler, J. N.; John, G. *Appl. Surf. Sci.* **1998**, *135*, 169–177.
(30) http://www.srdata.nist.gov/xps/.
(31) Sun, Y. B.; Hu, L. T.; Xue, Q. J. *Wear* **2009**, *266*, 917–924.
(32) De Barros, M.; Bouchet, J.; Raoult, I.; Mogne, Th.; Martin, J.; Kasrai, M.; Yamada, Y. *Wear* **2003**, *254*, 863–870.

AM900847J